



## OPEN Evaluation of the trunk modules in the symmetrical and three-dimensional asymmetrical trunk positions

Sharareh Kian-Bostanabad<sup>1</sup>, Mahmoodreza Azghani<sup>1✉</sup> & Mohammad Parnianpour<sup>2</sup>

Modularity (Muscle synergy) is the concept that has been used to answer the question of how the central nervous system (CNS) coordinates the body's high degrees of freedom. This study aimed to investigate the trunk muscle synergies in symmetrical and asymmetrical positions. Fourteen healthy males participated. Electromyographical activities of 16 muscles were recorded during maximum voluntary isometric contraction (MVIC) in six main directions with two repetitions and maximum voluntary isometric extension (MVIE) of the trunk in 23 different three-dimensional trunk positions. Muscle synergies were extracted separately using non-negative matrix factorization during MVIC (with one/two repetitions) and MVIE. The effect of position changes on synergies was investigated using response surface models and the Pearson correlation coefficient. The findings show that 6 synergies for 6 directions MVIC and 2 synergies for MVIE are suitable with the variance accounted for of  $99.65 \pm 0.65$  and  $94.14 \pm 1.59$ , respectively. Trial repetition does not affect the synergies. In Conclusion, during the same activity in different positions and trials, the synergy of the main activity is preserved. These show the stability of synergies and their dependence on the activity type. This stability may help to determine the main damage caused and provide appropriate treatment protocol for trunk injuries.

**Keywords** Muscle synergy, Asymmetrical positions, Non-negative matrix factorization, Modularity, Motor control, Trunk muscles

### Abbreviations

EMG	Electromyography
EO	External oblique
ES	Erector spinae
IL	Iliocostalis lumborum
IO	Internal oblique
LBP	Low back pain
LD	Latissimus dorsi
MF	Multifidus
MSE	Mean square error
MVIC	Maximum voluntary isometric contraction
MVIE	Maximum voluntary isometric extension
NMF	Non-negative matrix factorization
RA	Rectus abdominis
RSM	Response surface model
SP	Scalar product
VAF	Variance accounted for

Altered trunk motor control during multidirectional activities may be related to an increased risk of low back pain (LBP)<sup>1–3</sup>; As altered motor control for the lumbar spine has been reported in LBP patients<sup>4</sup>. In occupational contexts, asymmetrical activities (such as lifting with one hand) can alter the trunk motor control and apply asymmetrical load on the spine<sup>5,6</sup>. To compensate for the decreased mechanical stability in these asymmetrical

<sup>1</sup>Department of Biomedical Engineering, Sahand University of Technology, P.O. Box: 51335-1996, Tabriz, Iran.

<sup>2</sup>Department of Mechanical Engineering, Sharif University of Technology, Tehran, Iran. ✉email: azghani@sut.ac.ir

positions, simultaneous muscle activity increases<sup>7</sup>, which in turn can affect the vertebral column load, the joint stiffness, and the stress distribution at the joint level<sup>2</sup>.

Considering the body's multiple degrees of freedom, how the central nervous system (CNS) overcomes this issue is a fundamental question in neuroscience<sup>8</sup>. There are many theories in this field, including the theories of generalism and computational account of the mind<sup>9</sup>, modularity<sup>10</sup>, massive modularity<sup>11</sup>, and redeployment<sup>12</sup>. In general, a module is a computational device that is naturally selected, innate, domain-specific, and universal<sup>13</sup>. The comparison of the modular and non-modular models during upright reaching movements in 72 points shows that modular decomposition is more effective than its alternative, i.e., non-modular, in terms of data approximation, direction discrimination, and dimensionality reduction<sup>14</sup>. Also, neuromechanical principles and neural plasticity support the development of motor modules<sup>15</sup>. Movement modules (also known as muscle synergies) are the coordinated patterns of muscle activity that flexibly combine to create functional movement behaviors<sup>15</sup>. These modules are used by CNS to simplify task creation<sup>16</sup>. Therefore, during movement, instead of controlling individual muscles, the CNS controls muscle synergies or muscle groups that work at the same time<sup>17</sup>.

One method to test the hypothesis of muscle synergy is measuring motor behavior using muscle electromyography (EMG) and using factorization methods to define consistent features in EMG data across tasks<sup>18</sup>. A weighted set of muscle synergies is used to reconstruct the EMG signals, where each synergy is represented by its activation coefficients<sup>8,18</sup>. It is considered that the weights are independent of time, but their activation patterns are time dependent. Muscle synergies determine not only which muscles work, but also how they work together<sup>19</sup>.

Comparing the synergies of people with different nervous disorders (such as stroke, Parkinson's, etc.) shows that any disorder causes a specific change in muscle synergies<sup>20</sup>. Therefore, synergy extraction can be useful to determine the damage caused and provide suitable rehabilitation according to it<sup>20</sup>. Also, the studies showed that there is a difference in muscle synergy between healthy people and those with musculoskeletal injuries (difference in the number or change in the quality of extracted synergies)<sup>21–23</sup>. Therefore, synergy analysis is a promising approach for elucidating altered motor control that may facilitate the assessment and treatment of musculoskeletal injuries<sup>21</sup>.

Comparing the lumbar and abdominal muscle synergies in healthy people with those who feel recovered from lumbar injuries shows the differences in the extracted synergies between the two groups<sup>24,25</sup>. This suggests that a person's self-report of improvement or observation of their ability to perform tasks may not reflect post-injury changes. In this context, an objective examination of the muscle activity patterns provides more information that can help evaluate recovery and guide clinical decisions<sup>24,25</sup>.

For healthy people, a comparison of the lumbar muscle activity during different exertions in three anatomical planes shows that the force level (medium–high range) has an effect on the EMG amplitude, but does not change the recruitment patterns<sup>3,26,27</sup>. Examining the presence of muscle synergies in the trunk muscles during target matching tasks in the sagittal, transverse, and their combined positions was investigated by Sedaghat Nejad et al.<sup>18</sup>. They used the non-negative matrix factorization (NMF) method to extract the muscle synergies on a three-axial lumbar dynamometer. According to this study, four synergies are sufficient to reconstruct complex data sets of target-matching tasks. Eskandari et al. (2011) used an 18-muscle model at the L4/L5 level in a static state to extract the lumbar muscle synergies in three anatomical planes using NMF and reported the sufficiency of six synergies to access all points<sup>27</sup>. However, trunk muscle synergies in three anatomical planes have not been investigated using experimental tests. A similar process in the sagittal and coronal planes for the dynamic state shows that 77% of the lumbar muscle recruitment pattern can be restored by 4 synergies corresponding to the 4 directions of these planes<sup>28</sup>. These studies show the relationship between synergies and activity in the main movement planes and state the necessity of considering the functional role of synergy<sup>18</sup>. The mentioned studies have investigated the effect of different activities in the combined two/three-plane positions, while the effect of the position change during the constant activity on the trunk muscle synergies has not been investigated yet.

Our review shows trunk muscle synergies have not been investigated during activity in three main movement planes using experimental protocols. In addition, the issue of whether changing position during constant activity affects activity-related synergies has not been investigated. Therefore, this paper aimed to evaluate trunk muscle synergies during maximum voluntary isometric contraction (MVIC) in six main directions and maximum voluntary isometric extension (MVIE) activity in three-dimensional positions (due to its importance in lifting). Comparing the extracted synergies from these two modes can provide insight into the effect of position change on the concept of synergy. Also, checking the compatibility of synergies between subjects and their stability in the trial repetition is one of the goals of the present study. Considering the importance of the synergy concept in the biomechanical and clinical fields (mentioned above), these insights can help better understand synergy and its use in different situations. Relying on the synergy dependence on the activity type, it is expected that the main synergies will be preserved by changing the position and repeating the trial.

## Materials and methods

### Participants

14 male volunteers between the ages of 23–29 participated. Their mean age, weight, and height were  $25 \pm 2.5$  years,  $74 \pm 5.6$  (between 63 and 78) kg, and  $177 \pm 4.56$  (between 162 and 180) cm, respectively. None of them had a history of LBP in the past year. The test conditions were explained to the subjects and their informed consent to participate was obtained. Any personal information was kept confidential. They could refuse to participate in the research at any time. Efforts were made to ensure that involvement in the research did not cause any harm to the subjects. The study was reviewed by Tabriz University of Medical Sciences and approved with the ID IR.TBZMED.REC.1400.312 ethics code.

## Device and data collection

Before the test, a familiarization session was held for the subjects. On the test day, after preparing the lumbar and abdominal skin (cleaning with alcohol and shaving), EMG surface electrodes (*eWave*®, Iran) were installed on the right and left sides on the external oblique (EO), rectus abdominis (RA), internal oblique (IO), erector spinae (ES) at the L2 level, iliocostalis lumborum at the distances of the 3 and 6 cm (IL3, IL6), latissimus dorsi (LD) and multifidus (MF)<sup>29</sup>. For the RA, the electrodes were placed 1 cm above the umbilicus and 2 cm lateral to the midline. For the EO, the electrodes were placed just below the rib cage and along a line connecting the most inferior point of the costal margin and the contralateral pubic tubercle. For the IO, the electrodes were placed 1 cm medial to the anterior superior iliac spine and beneath a line joining both anterior superior iliac spines. For the LD, the electrodes were placed over the muscle belly at the T12 level and along a line connecting the most superior point of the posterior axillary fold and the S2 spinous process. For the ES and IL muscles at a distance of 3 and 6 cm, electrodes were aligned parallel to the line between the posterior superior iliac spine and the lateral border of the muscle at the 12th rib. For the MF, the electrodes were placed at L5 and aligned parallel to the line between the posterior superior iliac spine and the L1–L2 interspinous space<sup>29</sup>. In this study, a triaxial lumbar dynamometer (Sharif Lumbar Isometric Strength Tester<sup>30</sup>) was used to record torques and positions in three main movement planes. Subjects were placed inside the dynamometer in a standing position and fixed by appropriate fasteners. Using the foot pedestal, his height (the distance of the subject from the ground) was adjusted so that the axis of the device passed through the L5/S1 joint. In the beginning, each subject was asked to exert MVIC 12 times (2 times in each of six directions of flexion, extension, right and left lateral bending and rotation) in the upright standing. After that, the MVIE was performed in 23 different anatomical positions. The angles included 0°, 15°, 30° and 45° in the sagittal, −15°, 0° and +15° in the transverse, and 0° and −15° in the coronal plane. Combined and single-plane modes for MVIE include 23 positions: 3 in the sagittal (15°, 30°, 45°), 2 in the transverse (−15°, +15°), 1 in the coronal (−15°), 6 in the sagittal-transverse ((15°, −15°), (30°, −15°), (45°, −15°), (15°, 15°), (30°, 15°), (45°, 15°)), 3 in the sagittal-Coronal ((15°, −15°), (30°, −15°), (45°, −15°)), 2 in the coronal-transverse ((−15°, −15°), (−15°, 15°)), and 6 in the sagittal-coronal-transverse planes((15°, −15°, −15°), (30°, −15°, −15°), (45°, −15°, −15°), (15°, −15°, 15°), (30°, −15°, 15°), (45°, −15°, 15°)). The order of trials was chosen randomly. Data collection in each trial included 5 s of activity with verbal encouragement and 2 min of rest time between trials for fatigue prevention<sup>31</sup>. The sampling rate of EMG data is equal to 1000 Hz and for torque data is equal to 100 Hz.

## Synergy extraction

Stable 3 s of main direction torque (3 s with the lowest standard deviation (SD)) and its equivalent EMG in each trial were selected and noise cancelation was done (band-pass filtered at 10–500 Hz). The steps mentioned in Fig. 1 were followed to prepare the normalized EMG and extract synergies. For each EMG signal, the mean value was subtracted from the data (referenced data). After that, the full wave rectification, 10 Hz low-pass filtering, and down sampling to have 200 samples were done for each signal. Finally, data normalization was done for each subject by dividing all data by the maximum of all trials for each muscle. The muscle synergies were extracted using the NMF method<sup>32,33</sup>. In this method, the EMG matrix with *j* rows (number of muscles) and *i* columns (number of data) is created for each subject (matrix *M*). The NMF algorithm is used to decompose this matrix into two separate matrices: matrix of muscle modules *W* with *j* rows and *N* columns (number of modules), and matrix of activation coefficients *C* with *N* rows and *i* columns. This method works by starting from a random value and iteratively updating the values until reaching the minimum error between the original and reconstructed matrices (Eq. 1).

$$M_{(j \times i)} = W_{(j \times N)} \times C_{(N \times i)} + \text{error} \quad (1)$$

Figure 1 shows the steps taken to extract muscle synergies.

## MVIC activities in six main directions

Muscle synergies for MVIC in 6 main directions were investigated using one and two repetitions (6 and 12 trials). For this purpose, the maximum torque out of two repetitions was selected for each direction. EMG data from the trials with maximum torque in 6 main movement directions were used to extract synergies in 6 trial modes. Once again, synergy extraction was done using both repetitions of MVIC trials to evaluate the effect of trial repetition. For this purpose, EMG data from all 12 trials was used to extract synergy. Due to the random order of the trials for each subject, in the analysis stage, the trials were arranged in the same order for all subjects for the possibility of interpreting the results.

The EMG matrix of each subject (contains 16 rows (muscle) in 1200 columns (6 trials × 200 data for each trial) for the 6-trial mode and 16 rows (muscle) in 2400 columns (12 trials × 200 data for each trial) for the 12-trial mode) was entered into the non-negative matrix factorization (nnmf) algorithm in MATLAB R2018a (<http://www.mathworks.com>) software and the muscle synergy vectors (*W*) and their activation coefficients (*C*) were calculated using the alternating least squares (als) algorithm for 1–16 synergy numbers. Then, the similarity between the synergy vectors and their activation coefficients for 6 and 12 trials were analyzed using the global (by all trials and muscles) and local (by trials or muscles) variance accounted for (VAF) and Pearson correlation coefficient (*R*<sup>2</sup>). VAF is defined as follows<sup>34–36</sup>:

$$VAF = 1 - \frac{\sum_{i=1}^p \sum_{j=1}^n (e_{i,j})^2}{\sum_{i=1}^p \sum_{j=1}^n (E_{i,j})^2} \quad (2)$$

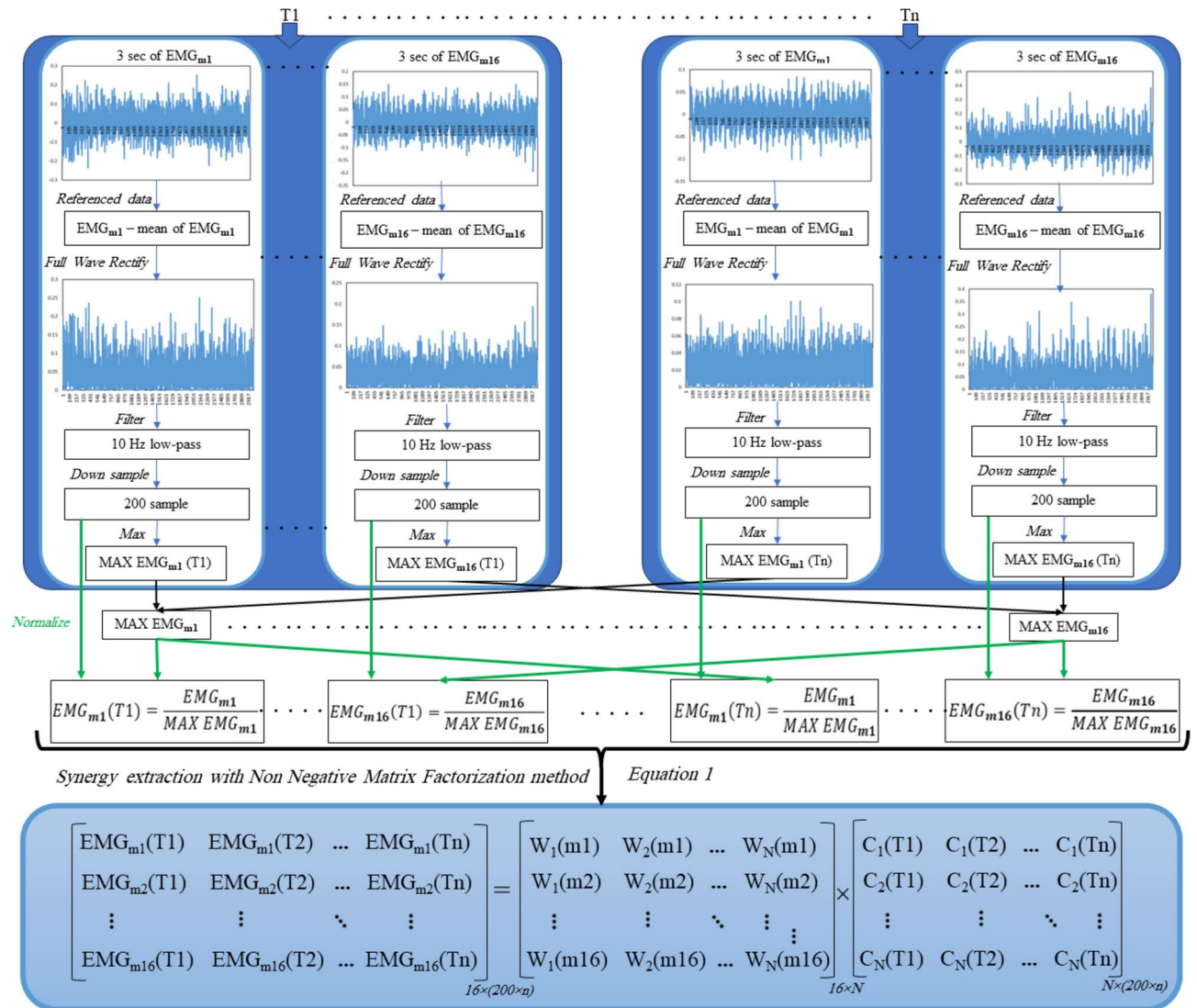


**Fig. 1.** The process of preparing electromyography (EMG) signals and extracting muscle synergies for 16 lumbar and abdominal muscles using the non-negative matrix factorization method during MVIC in six main directions and MVIE in different anatomical positions. Abbreviations: m: muscle (16 muscle), T: trial, n: number of trials (6 and 12 for MVIC and 23 for MVIE), N: number of synergies (1–16 synergy), W: synergy vectors and C: synergy activation coefficients.

where  $p$  and  $n$  are the EMG matrix rows and columns, respectively,  $e$  is the error between the original and reconstructed EMG and  $E$  is the original EMG.

Finally, all subject's data were placed inside a single matrix and synergies were extracted. To this end, the mean value for each subject in each trial was used (16 rows (muscle) in 84 columns (14 people  $\times$  6 trials) for 6 trials and 16 rows (muscle) in 168 columns (14 subject  $\times$  12 trials) for 12 trials).

#### MVIE activity in different anatomical positions

Similar to the previous section, EMG signals were prepared and the NMF method was used (Fig. 1). The EMG matrix for each subject includes 16 rows (muscles) in 4600 columns (23 trials  $\times$  200 data for each trial) for each person. Finally, the EMG matrix for all subjects with 16 rows (muscles) in 322 columns (14 subject  $\times$  23 trials) was used for synergies extraction.

To determine the optimum synergy number (from 1 to 16) for MVIC and MVIE, the criteria of global VAF  $> 90$ ,  $R^2 > 80$ ,  $\Delta VAF < 5$ ,  $\Delta R^2 < 5$  (adding one more synergy increases VAF and  $R^2$  by less than 5%), mean square error (MSE)  $< 5 \times 10^{-5}$  were used (Fig. 2)<sup>18,29,32–34,34,37</sup>. After that, local VAF and  $R^2$  by muscle and trial were calculated for each subject to ensure the optimality of the selected synergies. Figure 2 shows the flowchart of data analyzing steps.



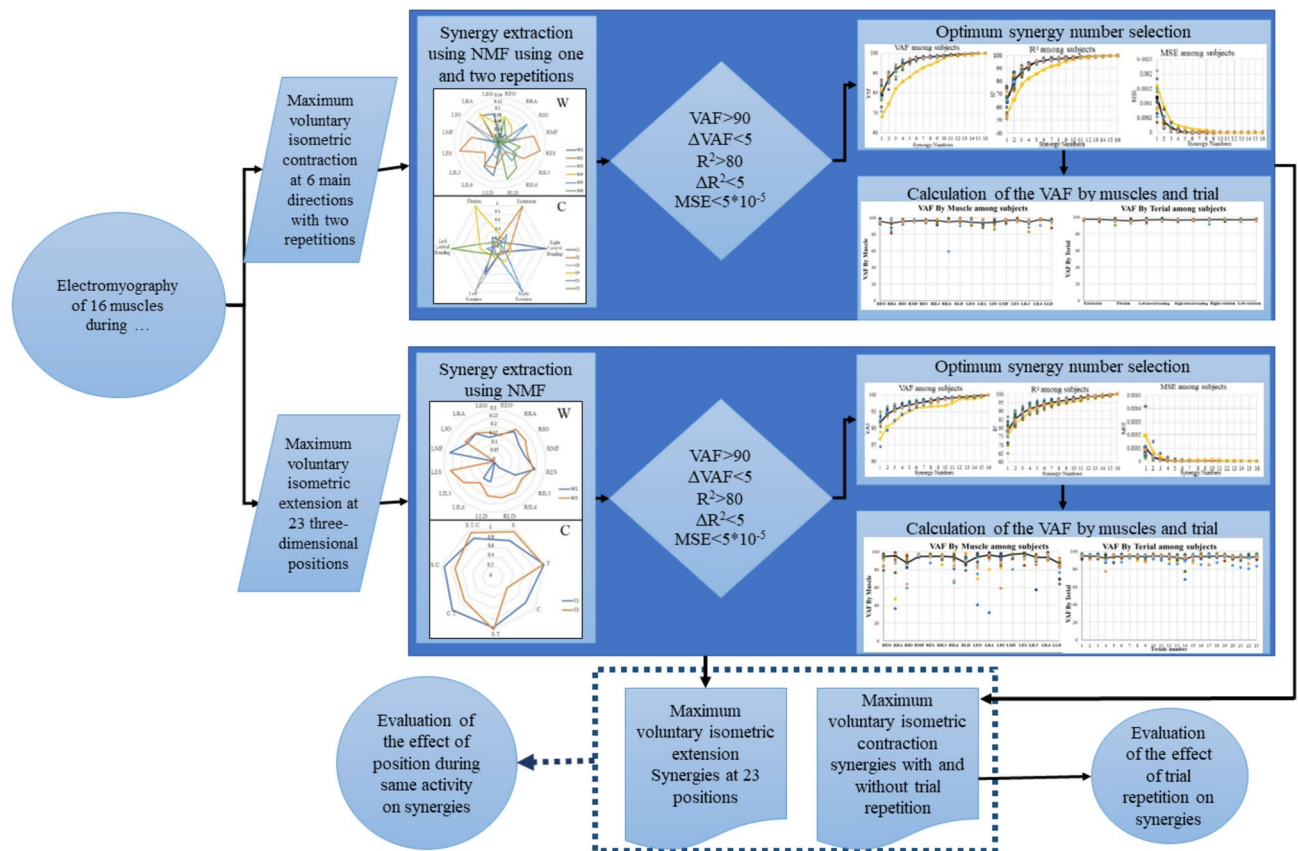


**Fig. 2.** Data analyzing steps. Synergies were extracted for 16 lumbar and abdominal muscles in two steps using non-negative matrix factorization (NMF). The optimum number of synergies was determined using variance accounted for (VAF), Pearson correlation coefficient ( $R^2$ ), and mean square error (MSE) and evaluated by the local VAFs. The extracted synergies from the two steps were compared using the Pearson correlation coefficient and response surface models.

### Validation of the extracted synergies

To check the synergies similarity between the subjects and their validation, two methods proposed in the literature were used: using the Scalar Product (SP) coefficient and reconstructing the EMG data using constant C and W.

#### Scalar product

In this method, the similarity between synergy vectors was checked using SP<sup>38</sup>. At first, the synergy vectors of all subjects are grouped in  $W_1, W_2, \dots, W_N$ . In each synergy, the similarity between pairs of subjects is calculated using SP. The mean of the calculated SP values gives the SP value for each synergy. SP was calculated for the extracted synergies from MVIE and MVIC, separately. Figure 3 shows how to calculate SP.

#### EMG reconstruction using constant W and C

In the first step, one subject's W (synergy vectors) were used to reconstruct the EMG data of other subjects in the NMF algorithm, and the new C matrix was calculated. The global VAF was calculated between the newly reconstructed EMG matrix (using constant W and new C, Eq. 1) and the original EMG of each subject. The second step is similar to the first one with the difference that C is kept constant. These two steps were calculated for pairs of subjects ( $13 \times 14$ ) for MVIC at six directions as well as MVIE at different positions<sup>34,35,39</sup>. This method calculation process is shown in Fig. 4.

### The relationship between MVIC and MVIE synergies

Pearson correlation coefficient was calculated between the synergies from the MVIE and 6 directions MVIC (all of 12 trials). Also, the response surface model (RSM) was used to present the relationship between them. For this purpose, the synergies of MVIE are dependent variables, and the synergies of MVIC in 6 directions are independent variables. To have a comprehensive model for all subjects, the Block effect was used. This model was presented for each synergy of MVIE, separately. RSM models were defined in the form of Eq. 32 as follows:

$$W_i = \beta_0 + \beta_1 W_{Flx} + \beta_2 W_{Ext} + \beta_3 W_{LLB} + \beta_4 W_{RLB} + \beta_5 W_{RR} + \beta_6 W_{LR} + BE_{subject} + \varepsilon; \quad i = 1, 2 \quad (3)$$

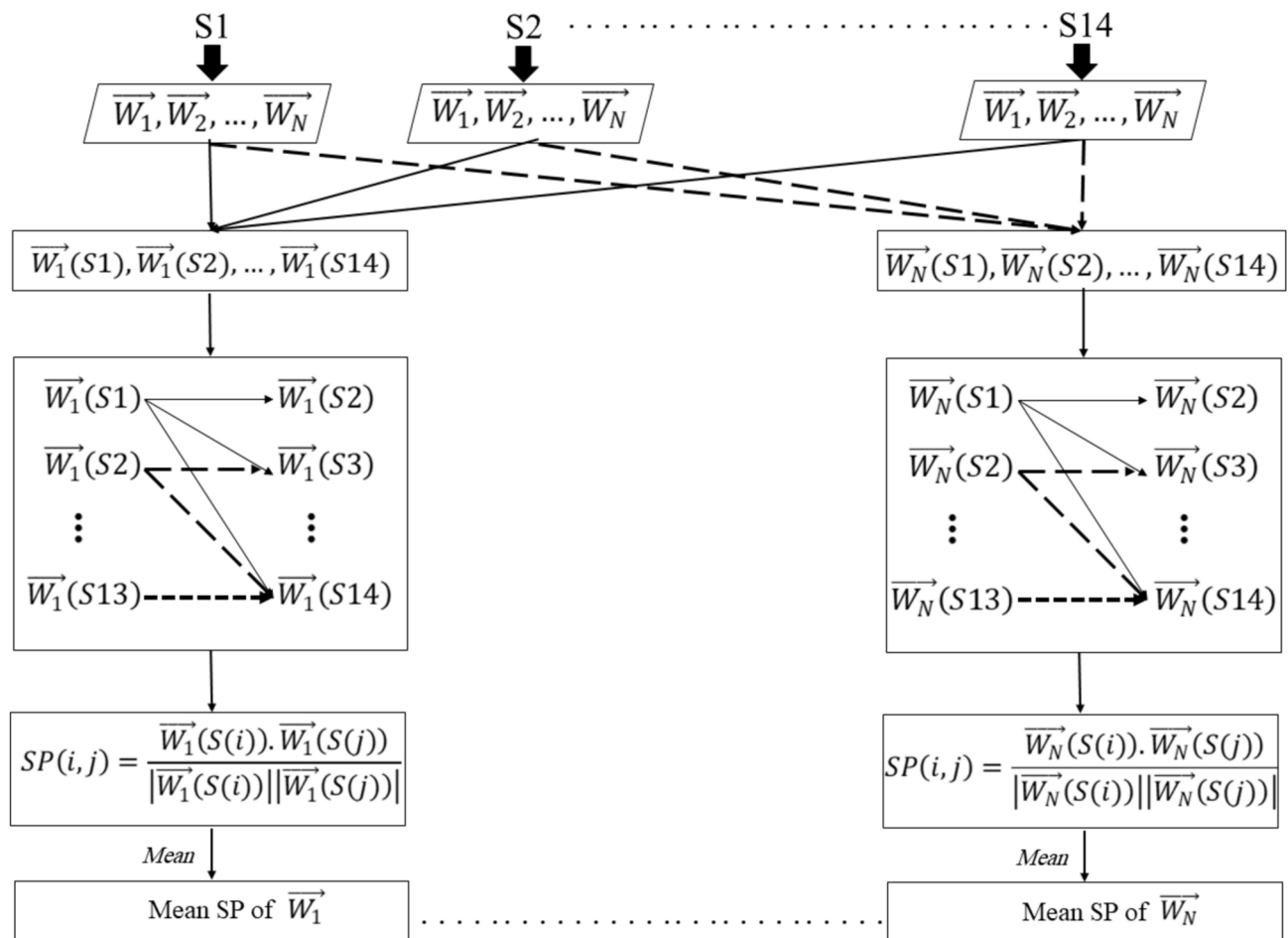


**Fig. 3.** Scalar Product calculation to check the synergies similarity between subjects. SP was calculated between pairs of subjects in each synergy. The mean of these SP values shows the similarity of the synergy. Abbreviations: S: subject (14), W: synergy Vectors, N: optimum synergy number, SP: scalar product,  $i$  and  $j$  are factors related to two subjects.

where  $\beta$ s are regression coefficients and  $W$  is synergy vectors. The subscripts are defined as: *Flx*: flexion, *Ext*: extension, *LLB*: left lateral bending, *RLB*: right lateral bending, *RR*: right rotation, *LR*: left rotation.  $i$  is equal to 1 to the optimum synergy number of MVIE.  $BE$  is the blocked effect (subjects) and  $\epsilon$  represents the error (For more information about the RSM method<sup>40</sup>).

Mathematical calculations were done in MATLAB R2018a (<http://www.mathworks.com>) software and statistical calculations were performed in Systat 13.1 (<http://grafiti.com>) software with the significance level of  $p < 0.05$ .

## Results

### Synergy extraction

#### MVIC activities in six main directions

According to the mentioned criteria in Fig. 2, 6 synergies are sufficient to reconstruct the EMG data in all 6 trials with mean global VAF and  $R^2$  of  $97.2 \pm 0.74$  and  $96.15 \pm 0.9$ , respectively. Also, 6 synergies are enough to reconstruct the EMG data in all of the 12 trials with mean global VAF and  $R^2$  of  $99 \pm 0.65$  and  $96.96 \pm 0.84$ , respectively. For all subjects at once, 6 synergies are enough to reconstruct EMG data in all 6 and 12 trials with global VAF and  $R^2$  equal to 90.69 and 89.11 for 6 trials and 91.3 and 89.76 for 12 trials, respectively.

The results of 12 trials are described below and the results of 6 trials are presented in Appendix A. Figure 5a shows the changes in global VAF,  $R^2$ , and MSE with synergy number (1–16) and the local VAFs by muscle and trial using 6 synergies.

According to Fig. 5a, the mean of local VAF by the muscle is between 93.19 and 98.14, and the mean of local  $R^2$  by muscle is between 89.11 and 95.09. Similarly, the mean of local VAF and  $R^2$  by trial are between 95.52 and 97.52 and 94.56 and 96.27, respectively.

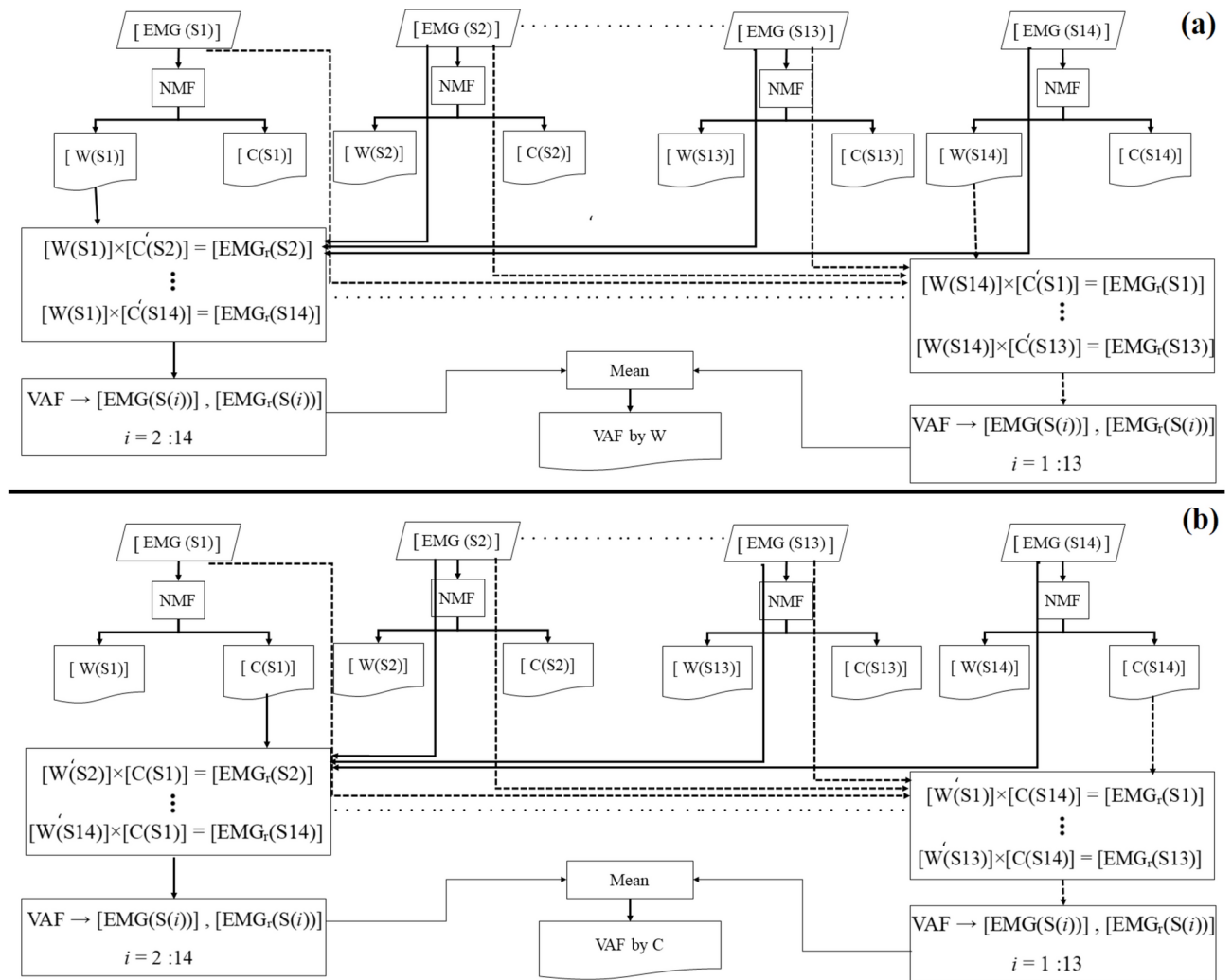


**Fig. 4.** The method of using (a) C and constant W and (b) W and constant C, to examine the synergies similarity between subjects. In this method, the EMG data of all subjects were reconstructed using W (a) and C (b) vectors of one subject. The global VAF was calculated between the reconstructed and original EMG matrix. Abbreviations: EMG: Electromyography, VAF: variance accounted for, NMF: non-negative matrix factorization,  $EMG_r$ : reconstructed EMG, S: subjects (14), W: synergy vectors, C: synergy activation coefficients, and  $i$  is the factor corresponding to subjects.

Figure 6a shows the polar plot of 16 muscle activities during 6 directions MVIC for one subject. Part (b) shows the extracted W and C vectors for the same subject. W vectors are plotted as percentages. About C, the mean value is calculated for each trial and each C is normalized to its maximum.

W along with C for 6 directions MVIC for all subjects are presented in Fig. 7. The left side graphs show the amount of participation of each muscle in each synergy, and the right side graphs show the activity of each synergy in each direction.

The mean of global VAF and  $R^2$  for W and C vectors between 6 and 12 trials are shown in Table 1.

The overall mean for global VAF and  $R^2$  of W is 73.02 and 76.06, respectively. Due to the different data numbers (1200 data for the 6-trial and 2400 data for the 12-trial), the mean values for each trial were used to compare the C vectors. The overall mean for global VAF and  $R^2$  of C is 76.68 and 75.89, respectively. The overall mean for local VAF and  $R^2$  by muscle is 74.89 and 75.13, respectively. Also, the overall mean for local VAF and  $R^2$  by trial is 76.71 and 79.17, respectively. Mean values for local VAF and  $R^2$  of each muscle and trial are given in Table A1 in Appendix A.

#### MVIE activity in different anatomical positions

After preparing EMG signals and extracting the synergies as mentioned in Fig. 1, the number of 2 synergies was selected according to the criteria of Fig. 2. Two synergies can reconstruct EMG data for 23 trials with the mean global VAF and  $R^2$  of  $94.1 \pm 14.59$  and  $85.43 \pm 3.18$ , respectively. About all subjects at once, 2 synergies are enough to reconstruct the EMG data in all 23 trials with global VAF and  $R^2$  equal to 90.33 and 82.84, respectively.

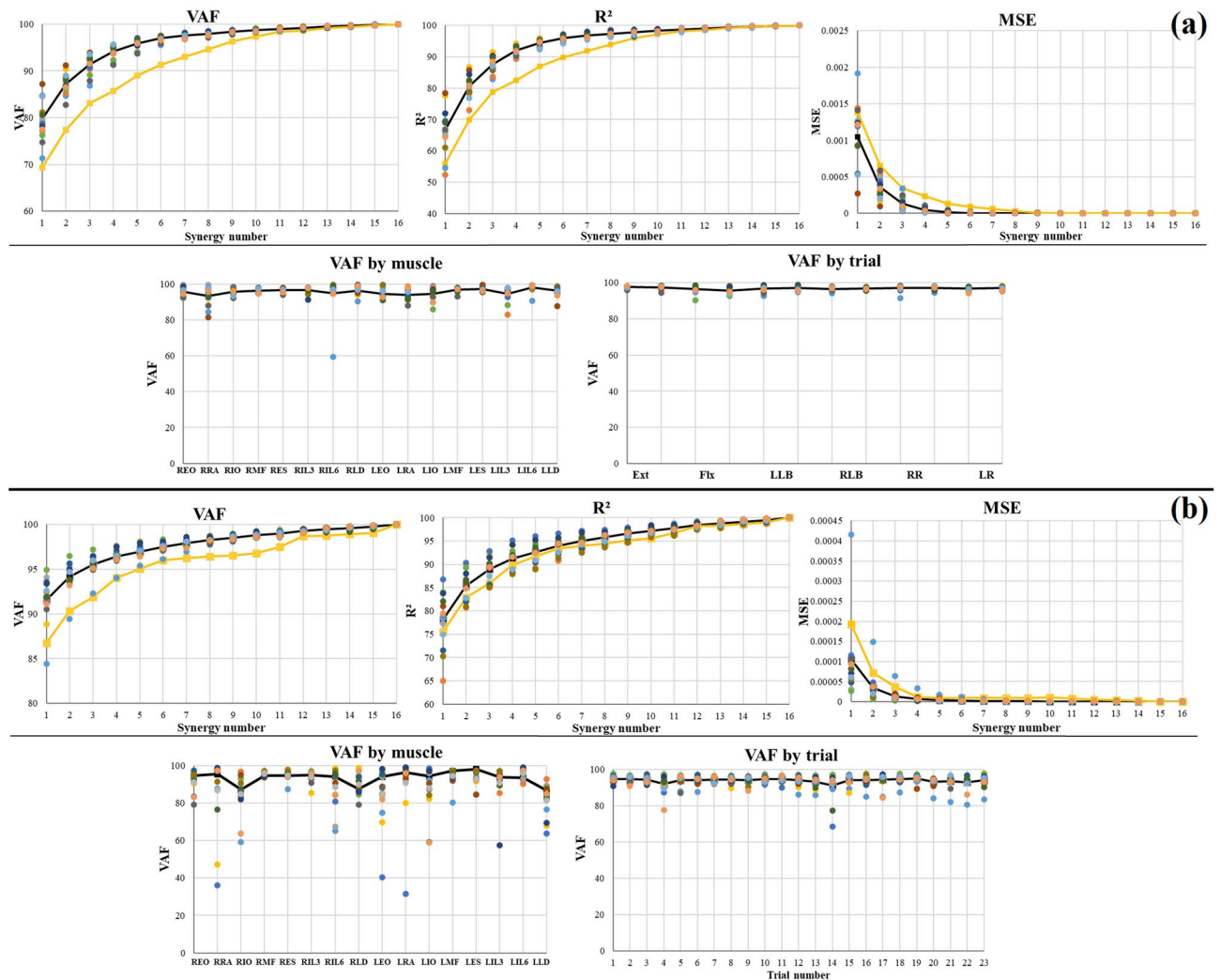


**Fig. 5.** Global variance accounted for (VAF), Pearson correlation coefficient ( $R^2$ ), and mean square error (MSE) according to the synergy number and Local VAF by muscle and trial (a) using 6 synergies for 6 main directions MVIC (Ext: extension, Flx: flexion, LLB: left lateral bending, RLB: right lateral bending, RR: right rotation, LR: left rotation) and (b) using 2 synergies for MVIE in 23 different positions. Each color corresponds to one subject and the black and yellow lines indicate the mean and all subject values, respectively. Muscle abbreviations: EO: external oblique, RA: rectus abdominis, IO: internal oblique, ES: erector spinae, IL: iliocostalis lumborum, LD: latissimus dorsi, MF: multifidus, R: right and L: left sides.

Global VAF,  $R^2$ , and MSE with synergy number as well as local VAF by muscle and trial using 2 synergies are shown in the Fig. 5b.

According to Fig. 5b the mean of local VAF is between 81.44 and 96.09 for 16 muscles and 91.18 and 94.98 for 23 trials. The mean of local  $R^2$  is  $84.1 \pm 1.65$  for muscles and  $67.54 \pm 8.42$  for trials.

Figure 8a shows the polar plot of W and C for one subject. About the C plot, to better discernment between asymmetrical positions, the mean value for each of the 23 trials was calculated and C was normalized to the maximum in each direction (7 directions). Figure 8b shows the W and C vectors for two synergies in all subjects. Sixteen synergy participation in two synergies are shown in the left graphs. The activity of each synergy in each trial (23 trials with 200 data for each one) is shown in the right graphs.

### Validation of the extracted synergies

The results of synergies evaluation using SP and EMG reconstruction using constant C and W are described below.

#### Scalar product

SP was calculated between W vectors according to Fig. 3 for pairs of subjects (91 states for each synergy). The mean values for both activities are shown in Table 2.



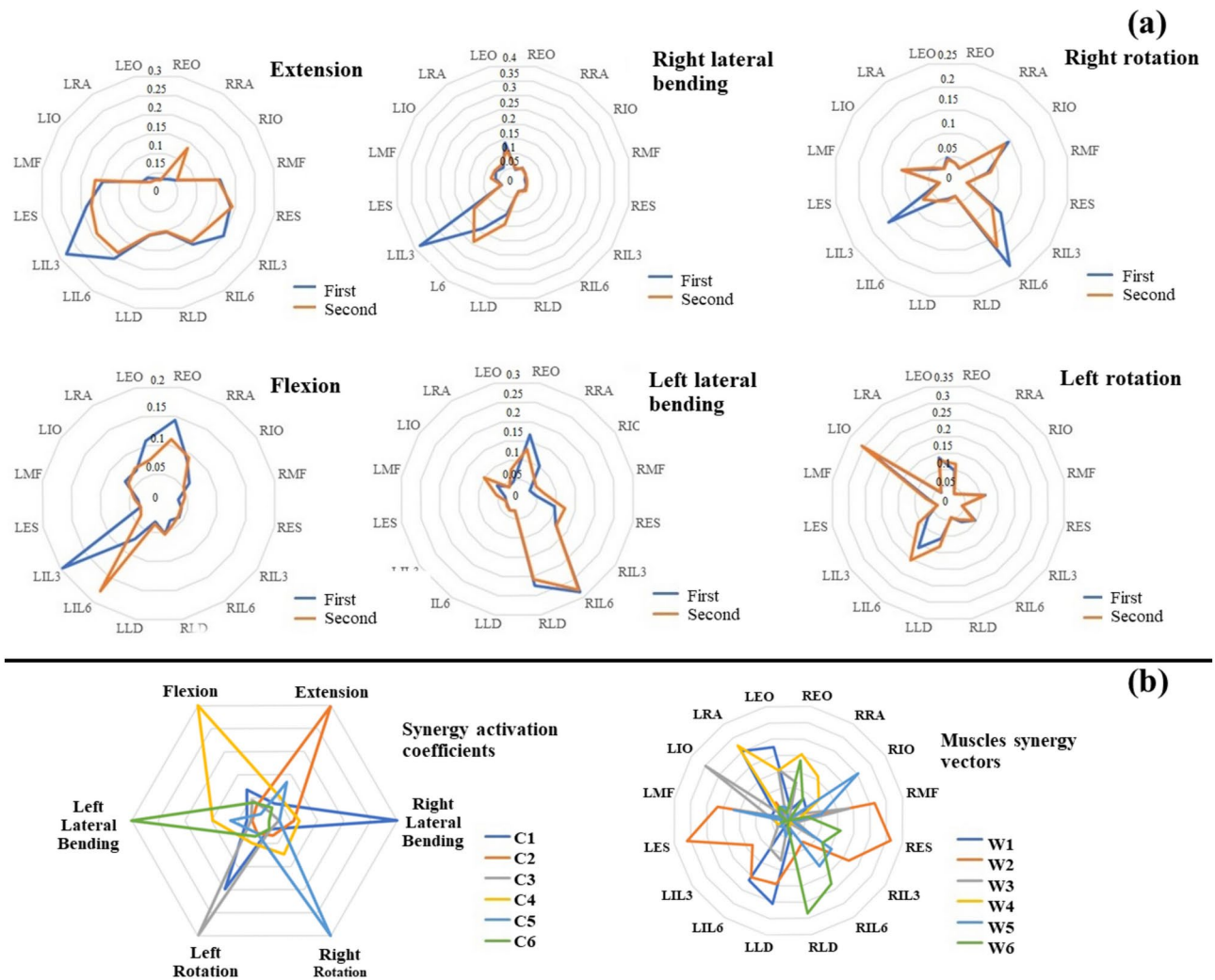


**Fig. 6.** (a) Polar plot of 16 muscle activities during MVIC in 6 main directions with two repetitions (two colors) and (b) Extracted synergy vectors (W) and their mean activation coefficients (C) for one subject (Subject 2). Muscle abbreviations: EO: external oblique, RA: rectus abdominis, IO: internal oblique, ES: erector spinae, IL: iliocostalis lumborum, LD: latissimus dorsi, MF: multifidus, R: right and L: left sides.

#### EMG reconstruction using constant W and C

Using this method (Fig. 4), the mean global VAF is  $65.99 \pm 16.97$  by constant W and  $83.75 \pm 5.75$  by constant C for MVIE in 23 different positions. Similarly, for MVIC in 6 directions, mean global VAFs are  $48.57 \pm 15.73$  and  $62.26 \pm 9.82$ , respectively.

#### The relationship between MVIC and MVIE synergies

Table 3 shows the RSM models obtained from Eq. 3. The relationship between synergy vectors of MVIC and MVIE along with their regression coefficients is shown in this table.

The correlation between synergy vectors is shown in Table 4. This table shows the Pearson correlation coefficient between 6 W of 6 main directions MVIC with 2 W of MVIE in different positions.

#### Discussion

This study aimed to investigate the lumbar and abdominal muscle synergies in symmetrical and asymmetrical positions and to check the consistency of synergies between subjects and their stability in the trial repetition and position changes. The results show the stability of synergies against different factors and their dependence on the type of activity.

#### Trunk modularity during MVIC activities in six main directions

The purpose of this analysis is to evaluate the muscle synergies for 6 main directions activities. According to the findings, 6 synergies are enough to reconstruct EMG data in all 12 trials with global VAF and  $R^2$  above 95. For some subjects, less than 6 synergies using some of the mentioned criteria seems sufficient, but using all criteria and considering the functional role of the extracted synergies<sup>18</sup> and the relationship between the

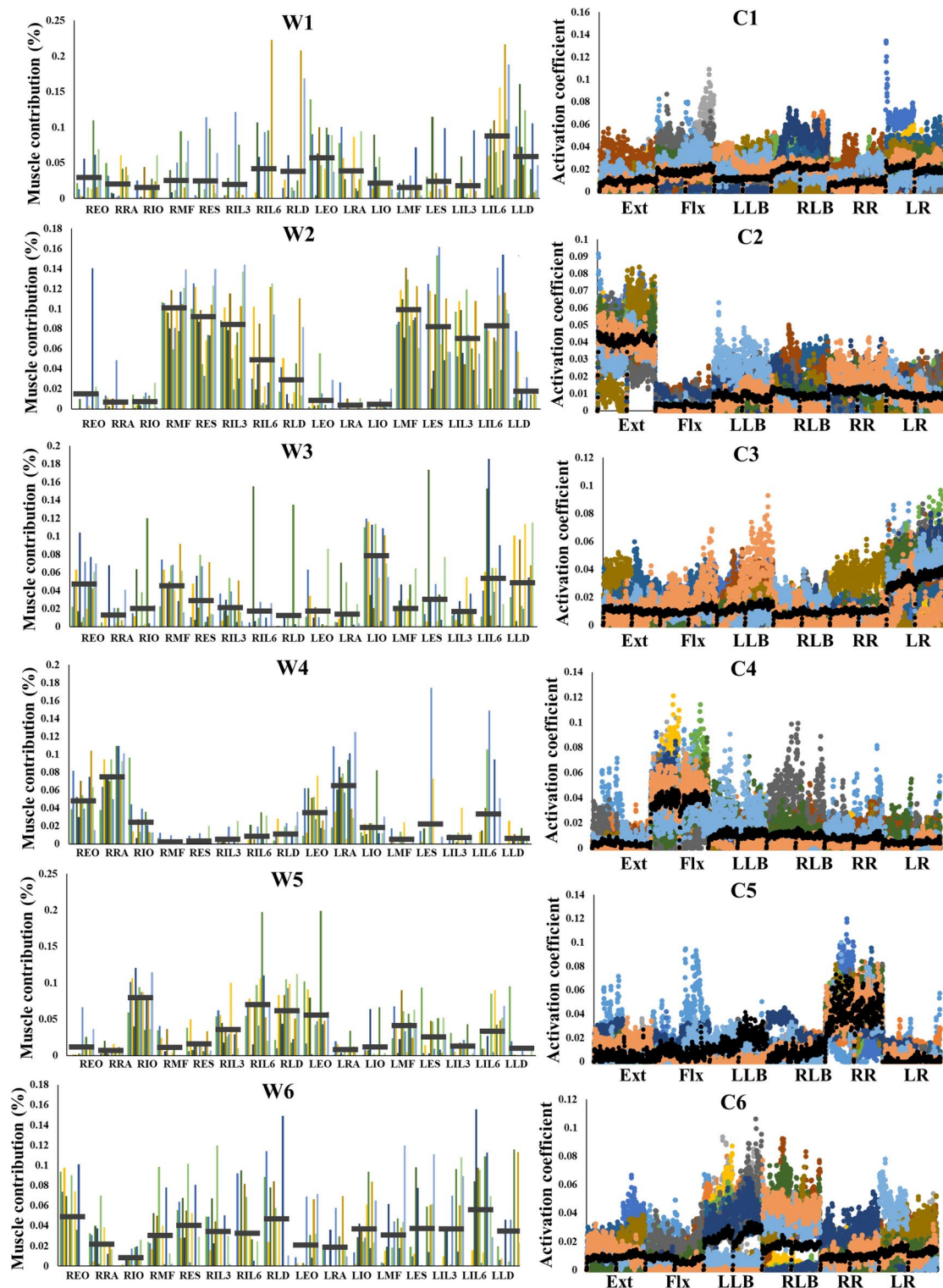


**Fig. 7.** Synergy vectors (W, left plots) and activation coefficients (C, right plots) of the 6 synergies for 6 main directions MVIC (Ext: extension, Flx: flexion, LLB: left lateral bending, RLB: right lateral bending, RR: right rotation, LR: left rotation). Each color corresponds to one subject and the black color indicates the mean values. Muscle abbreviations: EO: external oblique, RA: rectus abdominis, IO: internal oblique, ES: erector spinae, IL: iliocostalis lumborum, LD: latissimus dorsi, MF: multifidus, R: right and L: left sides.

		Synergy 1	Synergy 2	Synergy 3	Synergy 4	Synergy 5	VSynergy 6
W	VAF	74.76	78.69	70.57	69.12	78.28	66.71
	R <sup>2</sup>	79.28	78.75	74.43	69.22	83.52	71.14
C	VAF	73.86	80.83	77.15	68.28	79.46	80.48
	R <sup>2</sup>	58.51	84.51	77.51	65.57	84.31	84.92

**Table 1.** Mean of the global variance accounted for (VAF) and Pearson correlation coefficient (R<sup>2</sup>) for Synergy vectors (W) and activation coefficients (C) between extracted synergies for 6 main directions MVIC using one and two repetitions.

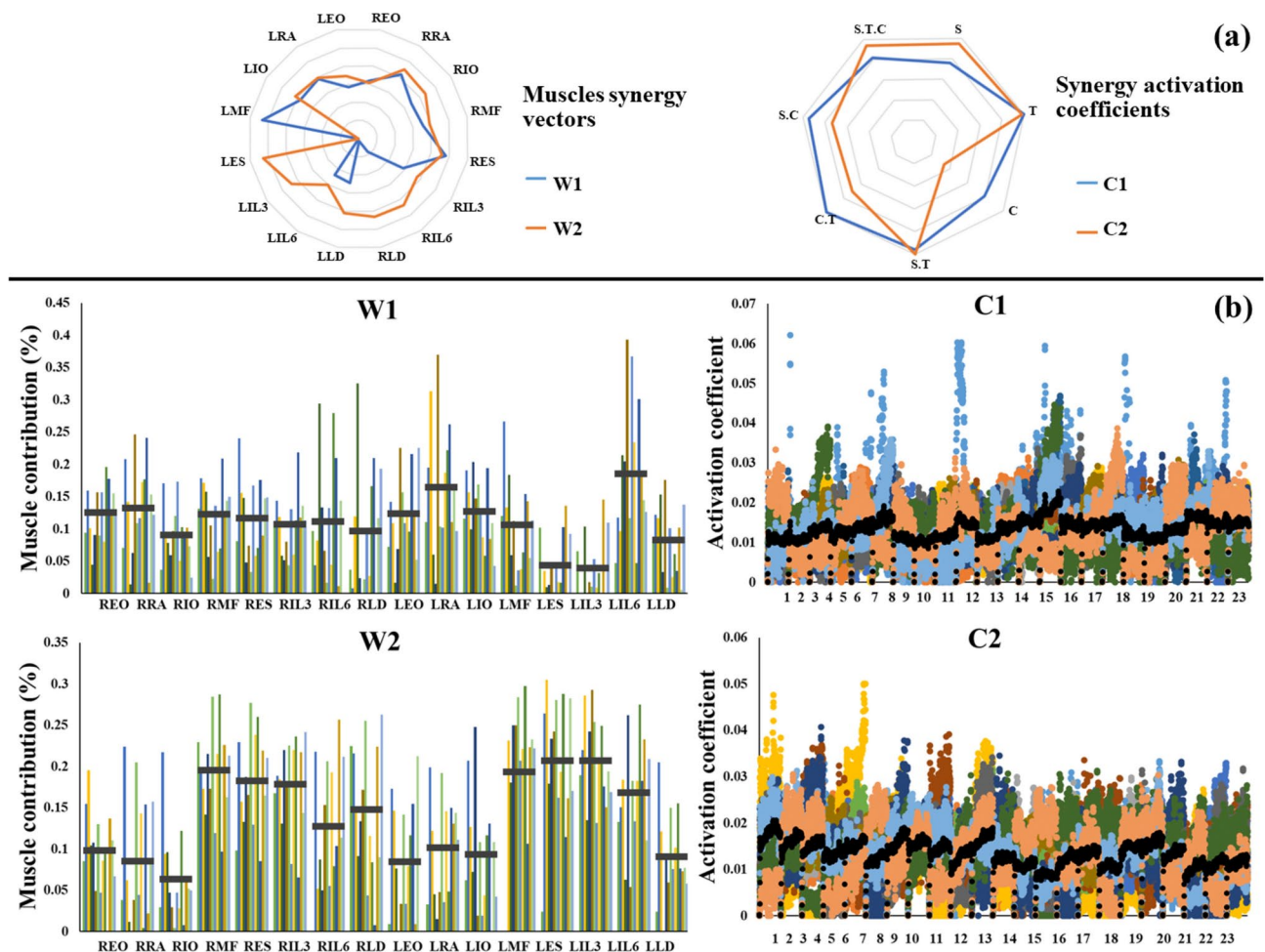


**Fig. 8.** (a) Polar plots of 2 extracted synergies (Synergy vectors (W) and mean activation coefficients (C)) for MVIE in different positions for one subject (Subject 2). To better discern between synergies behavior in the asymmetrical positions, 7 divisions were considered as follows: S: sagittal, T: transverse, C: coronal, S.T: sagittal-transverse, C.T: coronal-transverse, S.C: sagittal-coronal and S.T.C: sagittal-transverse-coronal. (b) W (left plots) and C (right plots) of 2 extracted synergies for MVIE at 23 different positions. Each color corresponds to one subject and the black color indicates the mean values. Muscle abbreviations: EO: external oblique, RA: rectus abdominis, IO: internal oblique, ES: erector spinae, IL: iliocostalis lumborum, LD: latissimus dorsi, MF: multifidus, R: right and L: left sides.

work goals and force demand to perform the desired activity<sup>17</sup> 6 synergies are selected for all subjects (each synergy for one direction). This finding is in accordance with the previous reports that 4 synergies correspond to the flexion, extension, right and left rotation for activity in the sagittal-transverse planes<sup>18</sup>, 4 synergies correspond to the flexion, extension, right and left lateral bending for activity in the sagittal-coronal planes<sup>28</sup> and 6 synergies correspond to the 6 main directions for activity in the sagittal-transverse-coronal planes using the biomechanical model<sup>27</sup> are sufficient. Our study advantage is the simultaneous examination of three anatomical planes using experimental tests. The local VAF and R<sup>2</sup> by muscle and trial for 6 synergies (Fig. 5a) confirm the

		MVIE in different positions		MVIC in 6 main directions					
		W <sub>1</sub>	W <sub>2</sub>	W <sub>1</sub>	W <sub>2</sub>	W <sub>3</sub>	W <sub>4</sub>	W <sub>5</sub>	W <sub>6</sub>
Scalar Product	Mean	0.776	0.858	0.824	0.496	0.498	0.57	0.64	0.694
	SD	0.094	0.08	0.098	0.186	0.278	0.23	0.236	0.135

**Table 2.** Mean (SD) of scalar product coefficient for comparing synergy vectors (W) between subjects.

$W_i = \beta_0 + \beta_1 W_{Flx} + \beta_2 W_{Ext} + \beta_3 W_{LLB} + \beta_4 W_{RLB} + \beta_5 W_{RR} + \beta_6 W_{LR} + B E_{subject} + \epsilon; i = 1, 2$									
Synergy	$\beta_0$	$\beta_1$	$\beta_2$	$\beta_3$	$\beta_4$	$\beta_5$	$\beta_6$	R <sup>2</sup>	%SEE
W <sub>1</sub>	6.777*	0.636*	0.045	0.138	0.311*	0.089	0.283*	0.248	0.176
W <sub>2</sub>	10.476*	-0.359*	0.830*	0.144	0.015	-0.119	0.055	0.470	0.205

**Table 3.** Response surface models for the relationship between the synergies of the MVIE and MVIC.  
\*Significant differences ( $p < 0.05$ ).

Synergy vectors		MVIE in different positions	
		W <sub>1</sub>	W <sub>2</sub>
MVIC in 6 main directions	W <sub>1</sub> (RLB)	0.485704	0.161945
	W <sub>2</sub> (EXT)	0.172299	0.931418
	W <sub>3</sub> (LR)	0.23462	0.077917
	W <sub>4</sub> (FLX)	0.489296	0.552963
	W <sub>5</sub> (RR)	0.102858	0.1591
	W <sub>6</sub> (LLB)	0.078587	0.459055

**Table 4.** Pearson correlation coefficients between 6 synergy vectors (W) of MVIC and 2 W of MVIE in different positions.

appropriateness of the selected synergies (local VAF by muscle > 75<sup>36</sup> and local R<sup>2</sup> by Muscle > 60<sup>35</sup> are considered optimal conditions).

According to Figs. 6 and 7, each of the 6 synergies has more activity in one direction than the other ones. Synergy numbers 2 and 4 are for extension and flexion, 5 and 3 are for right and left rotation, and 1 and 6 are for right and left lateral bending, respectively. Among the mentioned synergies, lateral bending synergies are less concentrated (show some activity in other directions, especially in the rotation direction), which can be due to the overlap between activities and its coupling effect, which was previously reported<sup>41</sup>. Also, according to W vectors in Fig. 7, high activity for flexor muscles during flexion and for extensor muscles during extension is observed. About asymmetrical activities (rotation and lateral bending), more muscles are activated with almost the same range (without the dominance of one or several muscle activities). This result is consistent with our previous findings<sup>42</sup>. Using the muscle co-contraction index in the previous study, we showed that all three types of muscle coupling (back-back, abdominal-abdominal, and back-abdominal) have high co-contraction during rotation and lateral bending, while only back-back muscles for extension and abdominal-abdominal muscles for flexion show high contraction<sup>42</sup>. Also, previous observations stated that muscle co-contraction during axial rotation is higher than flexion and extension<sup>43</sup>. The correlation of synergies with functional tasks of the trunk may be useful in the selective evaluation of synergies during a specific activity.

**Does trial repetition affect synergies in trunk MVIC activities?**

The findings show that trial repetition does not affect the synergy number (6 synergies are sufficient for both 6 and 12 trials). Regarding the extracted synergies quality, the high VAF and R<sup>2</sup> values between the 6 and 12 trial synergies (Tables 1 and A1) indicate the high similarity and show that trial repetition has no great effect on the extracted synergies. Also, Perez et al. (2002) showed that movement repetition has no effect on the muscle activity pattern, and considering the cost of repeating trials, they suggested that a single trial is sufficient to provide a subject's muscle activity in response to a specific static load<sup>26</sup>. It should be noted that in the current study, the effect of trial repetition was investigated in the symmetrical position. Performing activities in more complex and asymmetrical positions may affect the results.

**Trunk modularity during MVIE activity in different anatomical positions**

To investigate the effect of position changes with constant activity on synergies, the relationship between the W for MVIE with W for 6 directions MVIC was calculated (Tables 3 and 4). RSM was used to check the significance



of these relationships. According to these models, there is a significant relationship between the  $W_2$  and  $W_{Ext}$  ( $p=0.000$ ) with the regression coefficient of 0.830. According to Table 4,  $W_2$  has a correlation of 0.931 with  $W_{Ext}$ . After extension, flexion and left lateral bending synergies show moderate correlation with  $W_2$  (0.553 and 0.459, respectively), which only the flexion relation is significant ( $p=0.012$  and  $\beta=-0.359$ ). On the other hand, the high activity of the extensor compared to flexor muscles in  $W_2$  (Fig. 8b) indicates the dominance of extension in the asymmetrical positions.  $W_1$  shows the highest correlation with flexion (0.459) and right lateral bending synergies (0.456) (Table 4) which both are significant ( $p=0.000$  and  $\beta=0.636$  for flexion and  $p=0.006$  and  $\beta=0.311$  for right lateral bending). These findings show that  $W_{Ext}$  is more dominant than others in the asymmetrical positions, however, flexion and lateral bending synergies also come into play (with less activity than  $W_{Ext}$ ) due to trunk bending. This finding is consistent with our previous studies in symmetrical<sup>44</sup> and asymmetrical<sup>42</sup> positions. The previous studies evaluated co-contraction between 120 muscle pairs in different positions. The advantage of using synergy analysis compared to co-contraction between two muscles is the possibility of a comprehensive examination of muscle behaviors simultaneously in different activities. Therefore, the synergy method can obtain a map of huge data sets in simple vectors form, which are computationally and analytically valuable. The present study shows that performing fixed activity in asymmetrical positions preserves the main synergy of the activity and in addition forms another synergy related to the coupling activities. The trunk motor control strategies are coordinated to selectively call the muscles based on their anatomical arrangement and mechanical advantages to respond to asymmetrical positions to maintain spine stability, which has been reported previously<sup>5</sup>.

### Validation of extracted synergies

Synergy extraction using all subject's data has the same result as individual subjects (yellow graphs in Fig. 5). In the present study, two methods were used for synergies validation and findings show a good correlation between subject synergies. This can indicate the consistent pattern of trunk muscle recruitment among subjects, which has also been reported in previous studies<sup>18,45</sup>. This agrees with the optimal control theory, which states that despite the redundancy of neuromuscular system, the muscle activation patterns in specific movements are uniform among subjects and trial repetitions<sup>45</sup>. It is valuable to evaluate neuromuscular strategies in some diseases<sup>46</sup>. Therefore, this may be used to check back injuries.

Most diagnostic techniques and clinical tests focus on gross motor functions and miss the ability to answer fundamental questions (i.e., why, what, and how) about a subject's impairments and their ability to improve<sup>47</sup>. For example, why does a rehabilitation treatment help some people but not others?<sup>20</sup> What movement strategies change as a result of recovery or treatment?<sup>20</sup> Therefore, muscle synergies can help to: diagnose movement disorders, evaluate the rehabilitation effect, develop therapies to increase neural plasticity and movement recovery<sup>19,20</sup>. In the present study, muscle synergy for simple trunk activities was presented for healthy subjects. Comparison of LBP subjects' synergies with them during these activities can help determine the damage mainly caused (such as the loss or combination of a synergy) and provide appropriate treatment.

Although muscle synergies extraction using NMF is a common and acceptable method, how the CNS can coordinate movements using these synergies is still unknown<sup>48</sup>. However, there have been studies to find the origin of modularity<sup>49,50</sup>, but the degree to which motor modules are decoded by neuromechanical structures or rapidly emerge from neuromechanical interactions is an open question.

### Synergy extraction and choosing optimum synergy number methods

The method of Fig. 1 was used for synergy extraction<sup>32,33</sup>. Due to the wide data, the advantage of this method is to use the sample down instead of the mean for each trial<sup>18</sup>. Synergy extraction using the mean for each trial was implemented in the present study and obtained similar results. However, to increase the accuracy and not rely on the mean, the sample down was used.

To determine the synergy number, the minimum number of synergies that overall VAF is above 90<sup>32,34,35,39</sup> and adding one more synergy increases it by less than 5%<sup>34</sup> is considered optimum.  $R^2$  is similar to VAF, but its threshold is lower<sup>35</sup>. For MSE, a straight line is drawn from each synergy number to the maximum (16) in the overall VAF diagram and the mean square error between the straight line and VAF curve was calculated<sup>37</sup>. The first synergy number that reduces the MSE value to less than  $5 \times 10^{-5}$  is the optimum<sup>18,34,37</sup>.

Various methods have been used in studies to select the appropriate synergy number, among them VAF > 90 has more applications<sup>32,34,35,39</sup>. In comparison between VAF and  $R^2$ , it should be noted that  $R^2$  calculates the sum of squares relative to the mean and is based on linear regression with offset, which only compares the curve shapes. VAF calculates the sum of squares relative to zero and is based on linear regression passing through the origin. VAF is preferred over  $R^2$  because, in addition to the high similarity between the curve shapes, the equality of the actual measurements is required to have a high VAF<sup>35</sup>. Therefore, VAF is a more accurate measure than  $R^2$  and it is emphasized more in the present study, although to ensure the optimality of the selected synergy,  $R^2$ , the difference between VAF and  $R^2$ , and MSE were also evaluated.

### Limitations of work

This study was conducted on healthy young males. A similar study on women, people with different age ranges, and people with low back disorders can be done. Due to the large number of trials, only one angle (15 degrees) in the coronal and transverse planes and one torque level (maximum effort) were examined. Similar studies can investigate the effect of angle in these two planes as well as the torque level. It was impossible to evaluate the activity of deep muscles due to using surface EMG electrodes. In addition, unwanted signals from surrounding muscles can affect EMG and thus the extracted synergies. To reduce this effect, we tried to minimize this error by using the bipolar arrangement of the electrodes and accuracy in determining the electrode location. Regarding synergy extraction, we used the NMF method to extract, and VAF, MSE, and  $R^2$  criteria to select the optimum



number of synergies. Other factorization methods (such as principal component analysis) and more limited criteria (for example, considering only the VAF) can affect the results.

# Conclusions

According to our observations and previous findings, MVIC activities in 3 anatomical planes need one synergy for each of the main directions of the movement plane (The present study and<sup>18,27,28</sup>). The extracted synergies are resistant to trial repetition and have good compatibility across subjects. The advantage of our study is to examine the same activity (MVIE due to its importance in lifting) in different positions, and the findings show that the synergy related to the main activity (extension) is preserved in all three-dimensional positions. This can show the synergy resistance against the position changes and its dependence on the performed activity. In addition, in asymmetrical positions, the second synergy related to coupling activities is formed to maintain the position and stability. In the present study, trunk muscle synergies during simple activities were presented for healthy subjects. Comparison of LBP subjects' synergies with them during these activities can help determine the damage mainly caused (such as the loss or combination of a synergy) and provide suitable treatment strategies.

# Data availability

The data can be provided upon request via mail's of corresponding author.

Received: 22 April 2024; Accepted: 22 January 2025

Published online: 05 March 2025

# References

1. Mousavi, S. J. et al. The effect of angle and level of exertion on trunk neuromuscular performance during multidirectional isometric activities. *Spine* **34**, E170–E177. <https://doi.org/10.1097/BRS.0b013e31818aec05> (2009).
2. Sheikhzadeh, A., Parnianpour, M. & Nordin, M. Capability and recruitment patterns of trunk during isometric uniaxial and biaxial upright exertion. *Clin. Biomech.* **23**, 527–535. <https://doi.org/10.1016/j.clinbiomech.2007.11.017> (2008).
3. Talebian, S. et al. The effect of exertion level on activation patterns and variability of trunk muscles during multidirectional isometric activities in upright posture. *Spine* **35**, 443–451. <https://doi.org/10.1097/BRS.0b013e3181bc34b5> (2010).
4. Hadizadeh, M. et al. The effect of chronic low back pain on trunk accuracy in a multidirectional isometric tracking task. *Spine* **39**, E1608–E1615. <https://doi.org/10.1097/BRS.0000000000000628> (2014).
5. Butler, H. L., Hubley-Kozey, C. L. & Kozey, J. W. Activation amplitude patterns do not change for back muscles but are altered for abdominal muscles between dominant and non-dominant hands during one-handed lifts. *Eur. J. Appl. Physiol.* **106**, 95–104. <https://doi.org/10.1007/s00421-009-0994-9> (2009).
6. Weston, E. B. et al. One versus two-handed lifting and lowering: lumbar spine loads and recommended one-handed limits protecting the lower back. *Ergonomics* **63**, 505–521. <https://doi.org/10.1080/00140139.2020.1727023> (2020).
7. Granata, K. P. & Wilson, S. E. Trunk posture and spinal stability. *Clin. Biomech.* **16**, 650–659. [https://doi.org/10.1016/S0268-0033\(01\)00064-X](https://doi.org/10.1016/S0268-0033(01)00064-X) (2001).
8. Flash, T. & Bizzi, E. Cortical circuits and modules in movement generation: experiments and theories. *Curr. Opin. Neurobiol.* **41**, 174–178. <https://doi.org/10.1016/j.conb.2016.09.013> (2016).
9. Cowie, F., Woodward, J. The mind is not (just) a system of modules shaped (just) by natural selection 312–334. (Blackwell, 2004).
10. Fodor, J. A., The modularity of mind. (MIT press, 1983).
11. Tooby, J. & Cosmides, L. The psychological foundations of culture. *Adapt Mind: Evolut. Psychol. Gener. Cult.* **19**, 19–136 (1992).
12. Anderson, M. L. The massive redeployment hypothesis and the functional topography of the brain. *Philos. Psychol.* **20**, 143–174. <https://doi.org/10.1080/09515080701197163> (2007).
13. Samuels, R. Evolutionary psychology and the massive modularity hypothesis. *Br. J. Philos. Sci.* **49**, 575–602. <https://doi.org/10.1093/bjps/49.4.575> (1998).
14. Hilt, P. M. et al. Spatiotemporal organization of whole-body muscle activity during upright reaching movements in various directions: modularity or not modularity?. *bioRxiv* **155085**(12), 20. <https://doi.org/10.1101/155085> (2017).
15. Bizzi, E. et al. Combining modules for movement. *Brain. Res. Rev.* **57**, 125–133. <https://doi.org/10.1016/j.brainresrev.2007.08.004> (2008).
16. Bizzi, E. & Cheung, V. C. The neural origin of muscle synergies. *Front. Comput. Neurosci.* **7**, 51. <https://doi.org/10.3389/fncom.2013.00051> (2013).
17. Ting, L. H. & McKay, J. L. Neuromechanics of muscle synergies for posture and movement. *Curr. Opin. Neurobiol.* **17**, 622–628. <https://doi.org/10.1016/j.conb.2008.01.002> (2007).
18. Sedaghat-Nejad, E. et al. Is there a reliable and invariant set of muscle synergy during isometric biaxial trunk exertion in the sagittal and transverse planes by healthy subjects?. *J. Biomech.* **48**, 3234–3241. <https://doi.org/10.1016/j.jbiomech.2015.06.032> (2015).
19. Torricelli, D. et al. Muscle synergies in clinical practice: Theoretical and practical implications. *Emerging Ther. Neurorehab.* **II**, 251–272. [https://doi.org/10.1007/978-3-319-24901-8\\_10](https://doi.org/10.1007/978-3-319-24901-8_10) (2016).
20. Ting, L. H. et al. Neuromechanical principles underlying movement modularity and their implications for rehabilitation. *Neuron* **86**, 38–54. <https://doi.org/10.1016/j.neuron.2015.02.042> (2015).
21. Liew, B. X., Vecchio, A. & Falla, D. The influence of musculoskeletal pain disorders on muscle synergies—A systematic review. *PLoS One*. **13**, e0206885. <https://doi.org/10.1371/journal.pone.0206885> (2018).
22. Saito, H. et al. Muscle synergy patterns as altered coordination strategies in individuals with chronic low back pain: a cross-sectional study. *J. Neuroeng. Rehabil.* **31**, 20–69. <https://doi.org/10.1186/s12984-023-01190-z> (2023).
23. Saito, H. et al. Direction-specific changes in trunk muscle synergies in individuals with extension-related low back pain. *Cureus* **16**, e54649. <https://doi.org/10.7759/cureus.54649> (2024).
24. Hubley-Kozey, C., Moreside, J. M. & Quirk, D. A. Trunk neuromuscular pattern alterations during a controlled functional task in a low back injured group deemed ready to resume regular activities. *Work* **47**, 87–100. <https://doi.org/10.3233/WOR-131689> (2014).
25. Moreside, J. M., Quirk, D. A. & Hubley-Kozey, C. L. Temporal patterns of the trunk muscles remain altered in a low back-injured population despite subjective reports of recovery. *Arch. Phys. Med. Rehabil.* **95**, 686–698. <https://doi.org/10.1016/j.apmr.2013.10.003> (2014).
26. Perez, M. A. & Nussbaum, M. A. Lower torso muscle activation patterns for high-magnitude static exertions: Gender differences and the effects of twisting. *Spine*. **27**, 1326–1335. <https://doi.org/10.1097/00007632-200206150-00016> (2002).
27. Eskandari, A. H. et al. Employing muscular and stability synergies to perform a desired task. *Iran. J. Biomed. Eng.* **5**, 257–273. <https://doi.org/10.22041/ijbme.2011.13163> (2011).

28. Rouchi, M. B., Davoudi, M. & Parnianpour, M. Evaluation of lumbar muscle synergy in flexion movement using time-varying muscle synergies. *Iran. J. Biomed Eng.* **13**, 177–187. <https://doi.org/10.22041/ijbme.2019.109726.1493> (2019).
29. Ng, J. K. F. et al. Effect of fatigue on torque output and electromyographic measures of trunk muscles during isometric axial rotation. *Arch. Phys. Med. Rehabil.* **84**, 374–381. <https://doi.org/10.1053/apmr.2003.50008> (2003).
30. Azghani, M. R. et al. Design and evaluation of a novel triaxial isometric trunk muscle strength measurement system. *Proc. Inst. Mech. Eng. H. J. Eng. Med.* **223**, 755–766. <https://doi.org/10.1243/09544119JEIM537> (2009).
31. Kian-Bostanabad, S., Azghani, M. R. & Parnianpour, M. Electromyography linear and non-linear analyzing to evaluation of the rest times adequacy between 30 lumbar extension tests for fatigue prevention. *Muscles Ligaments Tendons J.* **13**, 586–592. <https://doi.org/10.32098/mltj.04.2023.10> (2023).
32. Milosevic, M. et al. Muscle synergies reveal impaired trunk muscle coordination strategies in individuals with thoracic spinal cord injury. *J. Electromyogr. Kinesiol.* **36**, 40–48. <https://doi.org/10.1016/j.jelekin.2017.06.007> (2017).
33. Lee, D. D. & Seung, H. S. Algorithms for non-negative matrix factorization. *Adv. Neural Inf. Process.* **13**, 556–562 (2001).
34. Frère, J. & Hug, F. Between-subject variability of muscle synergies during a complex motor skill. *Front. Comput. Neurosci.* **6**, 99. <https://doi.org/10.3389/fncom.2012.00099> (2012).
35. Torres-Oviedo, G., Macpherson, J. M. & Ting, L. H. Muscle synergy organization is robust across a variety of postural perturbations. *J. Neurophysiol.* **96**, 1530–1546. <https://doi.org/10.1152/jn.00810.2005> (2006).
36. Matsunaga, N. et al. Muscle fatigue in the gluteus maximus changes muscle synergies during single-leg landing. *J. Bodyw. Mov. Ther.* **27**, 493–499. <https://doi.org/10.1016/j.jbmt.2021.05.013> (2021).
37. Cheung, V. C. et al. Central and sensory contributions to the activation and organization of muscle synergies during natural motor behaviors. *J. Neurosci.* **25**, 6419–6434. <https://doi.org/10.1523/JNEUROSCI.4904-04.2005> (2005).
38. Cheung, V. C. et al. Muscle synergy patterns as physiological markers of motor cortical damage. *PNAS* **109**, 14652–14656. <https://doi.org/10.1073/pnas.1212056109> (2012).
39. Hug, F. et al. Consistency of muscle synergies during pedaling across different mechanical constraints. *J. Neurophysiol.* **106**, 91–103. <https://doi.org/10.1152/jn.01096.2010> (2011).
40. Kian-Bostanabad, S. & Azghani, M. R. The relationship between RMS electromyography and thickness change in the skeletal muscles. *Med. Eng. Phys.* **43**, 92–96. <https://doi.org/10.1016/j.medengphy.2017.01.020> (2017).
41. Azghani, M. R. et al. Normative database of response surface method for human trunk extension in isometric mode. *Proc. Inst. Mech. Eng. H. J. Eng. Med.* **237**, 855–868. <https://doi.org/10.1177/09544119231177564> (2023).
42. Kian-Bostanabad, S., Azghani, M. R., Parnianpour, M. Evaluation of maximum voluntary isometric lumbar extension in three-dimensional positions. *Int. J. Occup. Saf. Ergo.* (2024).
43. Thelen, D. G., Schultz, A. B. & Ashton-Miller, J. A. Co-contraction of lumbar muscles during the development of time-varying triaxial moments. *J. Orthop. Res.* **13**, 390–398. <https://doi.org/10.1002/jor.1100130313> (1995).
44. Kian-Bostanabad, S., Azghani, M. R. & Parnianpour, M. Evaluation of the lumbar and abdominal muscles behavior in different sagittal plane angles during maximum voluntary isometric extension. *Proc. Inst. Mech. Eng. H. J. Eng. Med.* **238**(3), 301–312. <https://doi.org/10.1177/09544119231221896> (2024).
45. Todorov, E. Optimality principles in sensorimotor control. *Nat. Neurosci.* **7**, 907–915. <https://doi.org/10.1038/nn1309> (2004).
46. Krishnan, C. et al. Quadriceps and hamstrings muscle control in athletic males and females. *J. Orthop Res.* **26**, 800–808. <https://doi.org/10.1002/jor.20592> (2008).
47. Mancini, M. & Horak, F. B. The relevance of clinical balance assessment tools to differentiate balance deficits. *Eur. J. Phys. Rehabil. Med.* **46**, 239–248 (2010).
48. Amundsen Huffmaster, S. L. et al. Muscle synergies obtained from comprehensive mapping of the primary motor cortex forelimb representation using high-frequency, long-duration ICMS. *J. Neurophysiol.* **118**, 455–470. <https://doi.org/10.1152/jn.00784.2016> (2017).
49. Yokoyama, H. et al. Cortical correlates of locomotor muscle synergy activation in humans: An electroencephalographic decoding study. *iScience*. **15**, 623–639. <https://doi.org/10.1016/j.isci.2019.04.008> (2019).
50. Desrochers, E., Harnie, J. & Doelman, A. Spinal control of muscle synergies for adult mammalian locomotion. *J. Physiol.* **597**, 333–350. <https://doi.org/10.1113/JP277018> (2019).

## Author contributions

All authors contributed to the study's conception and design. Material preparation and data collection were performed by M.R.A. and M.P. Data analysis was performed by S.K.B. and M.R.A. All authors read and approved the final manuscript and agreed with the order of presentation of the authors.

## Funding

Funding was provided by Sahand University of Technology (Grant No. t1475).

## Declarations

## Competing interests

The authors declare no competing interests.

## Ethical approval

This study was performed in line with the principles of the Declaration of Helsinki. Approval was granted by the Ethics Committee of Tabriz University of Medical Sciences and approved with the ID IR.TBZMED.REC.1400.312 ethics approval number.

## Additional information

**Supplementary Information** The online version contains supplementary material available at <https://doi.org/10.1038/s41598-025-87802-1>.

**Correspondence** and requests for materials should be addressed to M.A.

**Reprints and permissions information** is available at [www.nature.com/reprints](http://www.nature.com/reprints).

**Publisher's note** Springer Nature remains neutral with regard to jurisdictional claims in published maps and institutional affiliations.

**Open Access** This article is licensed under a Creative Commons Attribution-NonCommercial-NoDerivatives 4.0 International License, which permits any non-commercial use, sharing, distribution and reproduction in any medium or format, as long as you give appropriate credit to the original author(s) and the source, provide a link to the Creative Commons licence, and indicate if you modified the licensed material. You do not have permission under this licence to share adapted material derived from this article or parts of it. The images or other third party material in this article are included in the article's Creative Commons licence, unless indicated otherwise in a credit line to the material. If material is not included in the article's Creative Commons licence and your intended use is not permitted by statutory regulation or exceeds the permitted use, you will need to obtain permission directly from the copyright holder. To view a copy of this licence, visit <http://creativecommons.org/licenses/by-nc-nd/4.0/>.

© The Author(s) 2025